Heliyon 9 (2023) e21498

Contents lists available at ScienceDirect

Heliyon

journal homepage: www.cell.com/heliyon

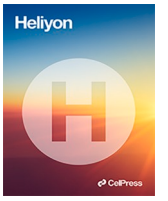

Targeting high performance of perovskite solar cells by combining electronic, manufacturing and environmental features in machine learning techniques

M. Mammeri [a], L. Dehimi [a], H. Bencherif [b,**], Mongi Amami [c], Safa Ezzine [c], Rahul Pandey [d], M. Khalid Hossain [e,*]

[a] LEPCM, Faculty of Science, University of Batna 1, Algeria
[b] LEREESI, HNS-RE2SD, Higher National School of Renewable Energy, Environment and Sustainable Development, Batna, 05078, Algeria
[c] Department of Chemistry, College of Sciences, King Khalid University, P.O. Box 9004, Abha, Saudi Arabia
[d] VLSI Centre of Excellence, Chitkara University Institute of Engineering and Technology, Chitkara University, Chandigarh, Punjab, 140401, India
[e] Institute of Electronics, Atomic Energy Research Establishment, Bangladesh Atomic Energy Commission, Dhaka, 1349, Bangladesh

ARTICLE INFO

Keywords:
Perovskite solar cell
Machine learning
Random forest technique
Prediction
Optimization

ABSTRACT

This study employs Machine Learning (ML) techniques to optimize the performance of Perovskite Solar Cells (PSCs) by identifying the ideal materials and properties for high Power Conversion Efficiency (PCE). Utilizing a dataset of 3000 PSC samples from previous experiments, the Random Forest (RF) technique classifies and predicts PCE as the target variable. The dataset includes various features encompassing cell architecture, substrate materials, electron transport layer (ETL) attributes, perovskite characteristics, hole transport layer (HTL) properties, back contact specifics, and encapsulation materials. ML-driven analysis reveals novel, highly efficient PSC configurations, such as Fe_2O_3/$CsPbBrI_2$/NiO-mp/Carbon, CdS/$FAMAPbI_3$/NiO–C/Au, and PCBM-60/Phen-NaDPO/$MAPbI_3$/asy-PBTBDT/Ag. Additionally, the study investigates the impact of crucial parameters like perovskite bandgap, ETL thickness, thermal annealing temperature, and back contact thickness on device performance. The predictive model exhibits high accuracy (86.4 % R^2) and low mean square error (1.3 MSE). Notably, the ML-recommended structure, SnO_2/CsFAMAPbBrI/Spiro-OmeTAD/Au, achieves an impressive efficiency of around 23 %. Beyond performance improvements, the research explores the integration of ML into the manufacturing and quality control processes of PSCs. These findings hold promise for enhancing conversion yields, reducing defects, and ensuring consistent PSC performance, contributing to the advancement of this renewable energy technology.

1. Introduction

Machine learning (ML) has recently garnered significant attention from researchers, driven by remarkable advancements in both mathematical models and computing capabilities [1]. ML techniques leverage specialized algorithms to learn from data, enabling the analysis, classification, and prediction of various phenomena [2]. While ML has demonstrated impressive performance across diverse

* Corresponding author.
** Corresponding author.
E-mail addresses: bencherif.hichem@hns-re2sd.dz (H. Bencherif), khalid.baec@gmail.com, khalid@kyudai.jp (M.K. Hossain).

https://doi.org/10.1016/j.heliyon.2023.e21498
Received 17 August 2023; Received in revised form 16 October 2023; Accepted 23 October 2023
Available online 25 October 2023

scientific domains, its application in materials science is a relatively recent development. In the realm of renewable energy, perovskite materials have emerged as a subject of intense interest, holding the potential to revolutionize the solar energy sector [3–8]. Notably, the power conversion efficiency (PCE) of Perovskite solar cells (PSCs) has witnessed a dramatic increase, surging from 2.2 % in 2006 to an impressive 26 % in 2023 [9]. Consequently, research endeavors have increasingly intertwined the development of PSCs with ML techniques, driven by the extensive accumulation of both experimental and computational data and the maturation of ML methodologies [10–12]. These studies harness ML techniques to elucidate the influence of specific materials and properties on solar cell devices, thereby paving the way for anticipatory design and optimization. In previous work, Mammeri et al. [13] reported on the impact of diverse combinations of materials, deposition methods, and storage conditions on the stability and efficiency of PSCs, harnessing the power of machine learning techniques. In this current study, we employ the supervised ML technique of Random Forest (RF) to investigate the optimal materials and structures conducive to achieving high PSCs PCE, offering clear guidelines for enhancing device performance. Additionally, our research unveils the pivotal factors affecting PCE, including the materials and thickness of the electron transport layer (ETL) and the materials and bandgap of the perovskite active layer (PAL). The RF model was trained using an extensive dataset comprising 3000 experimental samples of PSCs, reinforcing the model's reliability for providing actionable guidance in real-world experiments. However, the dataset collected for this study presents a challenge due to the presence of missing values and its high dimensionality, encompassing 35 distinct features. These features encompass various aspects of cell architecture, substrate materials, ETL (including materials, thickness, additives, deposition methods, and annealing temperature), perovskite (comprising composition of ions, materials, thickness, bandgap, annealing temperature, additives, deposition procedures, solvents, and anti-solvents), HTL (materials, thickness, additives, deposition), back contact (materials, deposition, thickness), and encapsulation materials. The dataset's high dimensionality poses a trade-off between model accuracy and computational efficiency [14].

To mitigate this challenge, we introduce correlation matrix analysis and feature engineering, specifically importance scoring, to retain the most relevant features while reducing computational complexity. Our analysis of PCE incorporates diverse material layers and properties, revealing novel configurations generated through ML techniques, such as Fe_2O_3/$CsPbBrI_2$/NiO-mp/Carbon, CdS/$FAMAPbI_3$/NiO–C/Au, and PCBM-60/Phen-NaDPO/$MAPbI_3$/asy-PBTBDT/Ag. Furthermore, we investigate the impact of influential parameters, including perovskite bandgap, ETL thickness, thermal annealing temperature, and back contact thickness, on device performance. Our findings highlight the promising potential of the proposed SnO_2/CsFAMAPbBrI/Spiro-OmeTAD/Au structure, boasting an impressive efficiency of 23 %.

2. Material and method

2.1. Dataset construction

The experimental data from published studies addressing the *PCE* of perovskite-based solar cells was screened to form the dataset utilized in the ML analysis. The Perovskite Database project [15], as well as other publications and reviews, provide the backbone of this dataset [10,11]. Data were carefully gathered while adhering to a number of guidelines. For instance, removing data from situations when the temperature is high or the light is intense.

2.2. Dataset description

Data are transformed into useful, practical insights using supervised machine learning. It makes it possible for researchers to make use of data to comprehend, decrease, or improve the desired results for their target variable. Throughout the training phase in the growth of the machine learning model, labeled input and output data are required for supervised machine learning. The training data is usually labeled by a data scientist during the building stage before being used to train and test the model. The model can be used to categorize previously undiscovered datasets and forecast outcomes once it has determined how the input and output data are related. This technique is referred to as supervised machine learning since it includes human supervision in some capacity [16]. The majority of the data offered is unlabeled, unprocessed data. For data to be adequately labeled and suitable for supervised learning, human input is typically necessary. Obviously, since a huge array of precisely labeled training data is required, this can be a costly operation.

The dataset used in this study contains 3000 samples of perovskite solar cells collected from different experimental studies. The utilized dataset is organized in Table 1. Each data relation with the cell component is organized as columns; for example, perovskite

Table 1
Data of Perovskite Solar cells used for Machine Learning training process.

Features (35) / Cells	ETL Materials	ETL Thickness (nm)	…	Perovskite	Bandgap (eV)	PCE (%)
Cell 1	TiO_2	40	…	FAMAPbBrI	1.73	12.1
Cell 2	SnO_2	80	…	MAPbI	1.61	8
Cell 3	PCBM60+BCP	220	…	MAPbI	1.61	13.06
……..	…….	…….	…	…	…….	….
Cell 2998	PCBM-60	120	…	CsAgBiBr	2.39	5.5
Cell 2999	TiO_2	70	…	MAPbI	1.61	17
Cell 3000	C60+BCP	80	…	CsPbBrI	2.07	9.6

materials, layers thicknesses, annealing temperature, and cell architecture, with 35 different columns. These columns (features) were introduced to the machine learning algorithm(model) as descriptors to train the model where each cell sample is organized as a row. The *PCE* of the cells is considered as target(output). The features used are cell architecture, substrate materials, ETL(materials, thickness, additives, deposition, annealing temperature), perovskite(composition a ions, b ions, c ions, materials short form, thickness, bandgap, annealing temperature, additives, deposition procedure, solvents,anti-solvents), HTL(materials, thickness, additives, deposition), back-contact (materials, deposition, thickness), encapsulation materials.

It is noticeable, that a number of the cell samples have one or more missing features. Instead of deleting these data points, two approaches are used to preserve the maximum of the data. For the categorical features (for example perovskite/ETL/HTL/BC materials ….), the missing values were replaced by a new category called "Unknown_material". For the numerical values (for example: bandgap, layer thickness …), a quite complicated approach was used, which can be summarized in Fig. 1.

Initially, taking the numerical features that contain missing values in different datasets and making a correlation matrix (method of Pearson) between these features and the PCE (see Fig. 2).

The features that have a relatively significant correlation with *PCE* to the original datasets are returned, and other features (irrelevant features) are deleted. One of these remaining features is selected as the target (it still contains missing values), and all rows (samples) that contain missing values of this target are deleted. The missing values (if any) of the other remaining numerical features are replaced by the mean value of the feature concerned. An evaluation of the accuracy is performed via training and testing the machine learning algorithm with this modification. It is noticeable that, if the accuracy is acceptable then predict the missing values of the deleted rows (in step 4), return these rows to the dataset, and restore the features that were replaced by the mean value to missing values. Finally, all the previous steps for each feature (perovskite bandgap, ETL thickness, ETL deposition thermal annealing temperature, back contact thickness) are repeated until all the missing values are fulfilled with the predicted value. Table 2 presents the precision of the prediction of the missing values for each feature.

2.3. Machine learning model construction

The initial dataset contains 35 different features which is not suitable for the model performance. Therefore, a feature selection technique was used. By using feature importance from RandomForestRegressor, from 35 features only 15 features have a relatively significant importance score to the PCE, the other features were deleted. See the importance score of the remaining features in Fig. 3 [17].

The accuracy of the model before the feature selection was 73.2 % using the R^2 method(the ideal value is 100 %) [18]. The GridSearchCV library was used to optimize the ML model hyperparameters [19]. Besides, the categorical encoder was employed to convert the categorical data to numerical data for the ML model. The accuracy of the model after feature engineering was 86.4 % using the R^2 method, and 1.3 using the mean square error (the ideal value is 0).

3. Results and discussion

To optimize the perovskite structure two approaches were used; first, optimizing the numerical values by predicting the *PCE* for different values in one feature while fixing the values of the other features (this operation has been done with 3 different proposed structures (Fe_2O_3/$CsPbBrI_2$/NiO-mp/Carbon (device 1), CdS/$FAMAPbI_3$/NiO–C/Au (device 2) and PCBM-60/Phen-NaDPO/$MAPbI_3$/asy-PBTBDT/Ag (device 3)). Second, optimizing the materials by predicting the *PCE* using all different materials under the same category and choosing the materials that recur in the highest PCE (these processes were applied to 3 different proposed structures). It is noticeable that we use existing materials in our data to form new PSC configurations to prevent the model overfitting of data [20]. The configurations used for the experience were generated using an algorithm that ensures no similarity with the training data, this

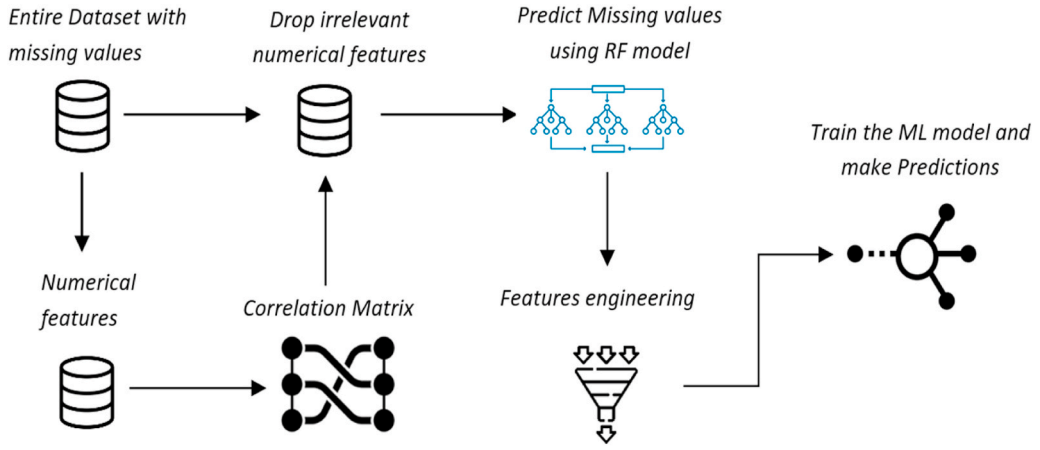

Fig. 1. Machine learning process workflow.

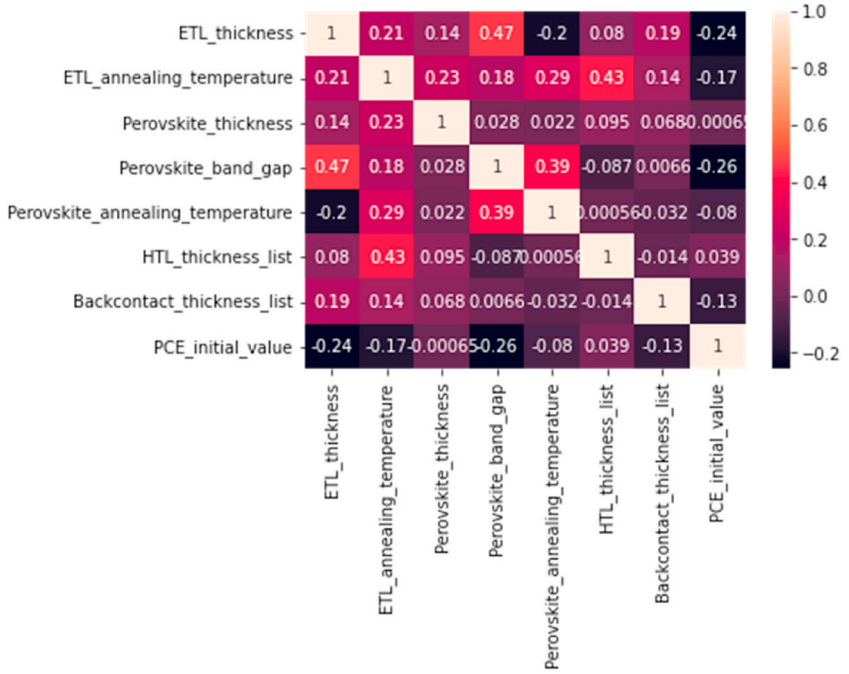

Fig. 2. Correlation matrix of numerical features.

Table 2
The accuracy of the predicted missing values.

Features	Number of the experimental values	Number of the predicted values	Accuracy of ML predictions
Bandgap	2102	898	87.9 %
ETL thickness	1268	1738	96 %
ETL annealing temperature	232	2768	98.5 %
BMC thickness	2472	528	98 %

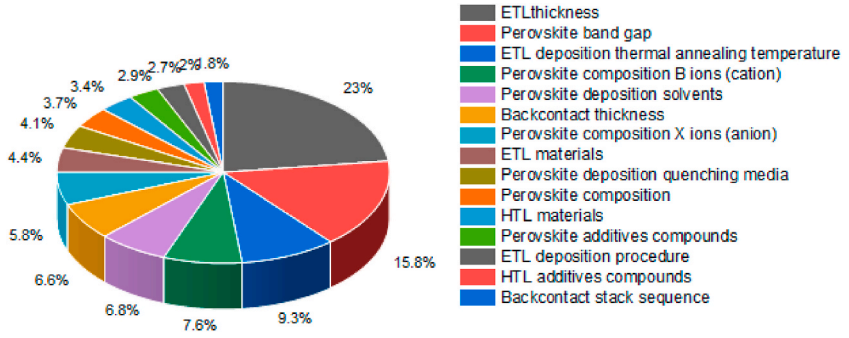

Fig. 3. The importance score of the remaining feature for the PCE.

prevents the ML model from biases the predictions toward samples in the training data. Moreover, using 3 different structures for each prediction allows a better generalization of the results. Which gives more reliability to the results.

The manufacture of perovskite solar cells uses a variety of experimental approaches, including vacuum deposition, fine inkjet printing, and solution-processed techniques including spin-coating, doctor-blade, and spray-coating. Perovskite materials may be deposited using several methods, each of which has unique benefits and allows for precise control over layer thickness. Perovskite solar cells are a viable choice for the production of clean and sustainable energy since researchers are constantly improving these methods to increase their stability and efficiency [21,22].

3.1. Perovskite material bandgap

The bandgap is a crucial characteristic of PV semiconductors, which describes what wavelengths of light the device can absorb and convert to electrical energy, it is obvious that a large band gap increases V_{OC} by lowering reverse saturation current, but it also inhibits device absorption, which lowers current. Therefore, an optimum band gap that can balance the compromise between J_{SC} and V_{OC} is required.

Fig. 4 shows the variation of the PCE against the perovskite absorber layer band gap for three structures. In this study, the domain of the bandgap variation is between 1.1eV and 3eV with a step of 0.01eV and the obtained optimum bandgap is between 1.55eV and 1.60eV. Additionally, numerous experimental findings demonstrate similar band gap ranges for optimum PCE. For instance, a PSC device including an active layer of CsFAMAPbI with a 1.6 eV band gap has recorded a high PCE of 22.77 % [23]. By using FAMAPbBrI | $(C_6H1_3NH_3)$PbI with a band gap of 1.56 eV, J. Yoo et al. reached a high PCE of 22.6 % [24]. Interestingly, Fig. 3 shows that the importance score of the bandgap is 15.8 % which is considered the highest importance score among all the 35 features used in this work. Which demonstrates the importance of the band gap for maximizing the device PCE.

3.1.1. ETL thickness

In perovskite solar cells (PSCs), the charge extraction function of electron transport layers (ETLs) is essential. The deposition of ETLs at low temperatures, even at room temperature, is particularly attractive for the production of flexible solar cells on polymer substrates.

The impacts of a high ETL thickness (>200 nm) include: (1) limiting electron transit to FTO; (2) increasing the recombination rate, which lowers V_{OC}; and (3) adding series resistance to the device's structure, which reduces the fill factor and cell efficiency.

Fig. 5 depicts the *PCE* variation against ETL material thickness for three structures. Herein, the ETL thickness domain is considered to be between 20 nm and 120000 nm with a 10 nm step. The obtained optimum ETL thickness via ML is between 140 nm and 170 nm which is suitable for efficient solar cells considering the aforementioned effect caused by thick ETL.

3.2. ETL thermal annealing temperature

ETLs for perovskite solar cells have been prepared using a variety of methods, including electro-deposition, sol-gel, and solution-processing of nanoparticles [21–25]. The solution approach is appealing in order to take benefit of the highly efficient production processes because the electro-deposition method is difficult. Owing to the considerable decomposition temperature of the precursor, the most popular solution processing ETL sol-gel technique necessitates thermal annealing at an elevated temperature, often above 200 °C, which prohibits the production of flexible solar cells. A lower manufacturing temperature remains desirable for flexible solar cells [26]. Fig. 6 depicts the *PCE* variation as a function of ETL thermal annealing temperature for three structures. For the ML calculation procedure, the thermal annealing temperature domain is taken between 25C and 550C with 5C as a step. The obtained results show that thermal annealing temperature doesn't follow any pattern, it seems like every material has its own optimum annealing temperature.

3.3. Back contact thickness

After illumination, the perovskite layer of typical perovskite solar cells produces electron-hole pairs. The cathode and anode, which are where the electron transport material (ETM) and the hole transport material (HTM), respectively, gather the electrons and holes,

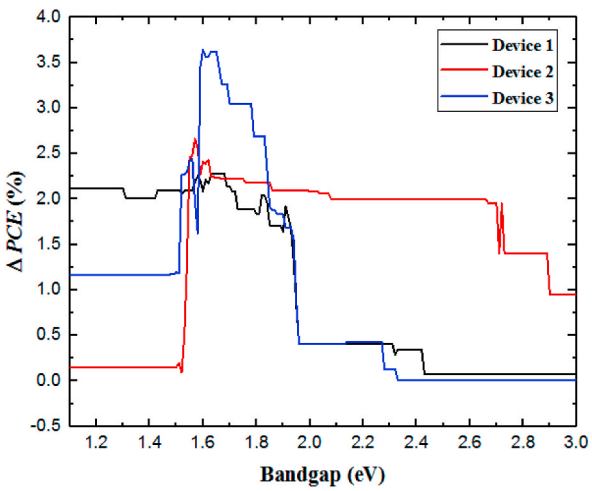

Fig. 4. *PCE* variation against perovskite material band gap.

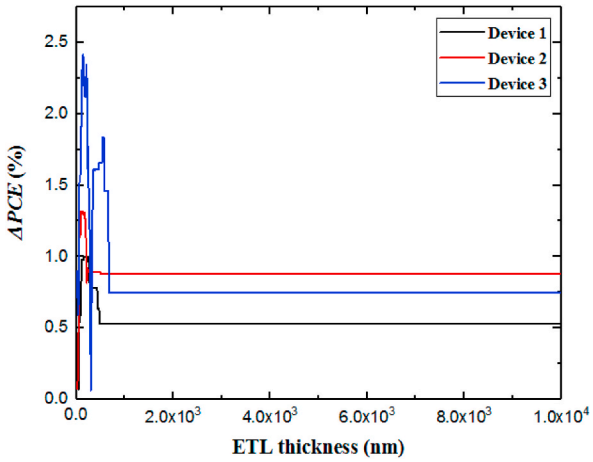

Fig. 5. *PCE* variation against ETL material thickness.

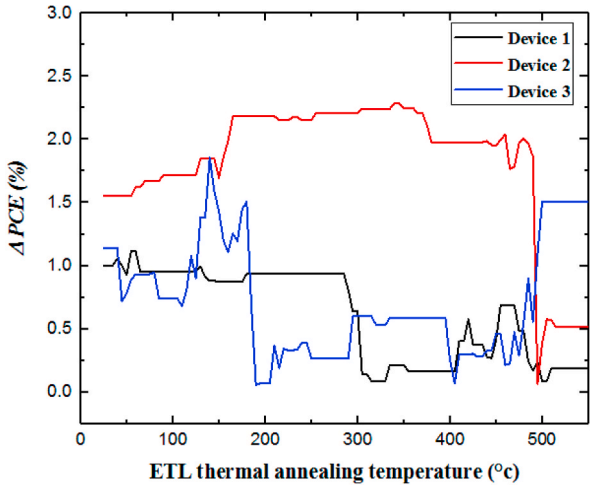

Fig. 6. *PCE* variation as a function of ETL thermal annealing temperature.

respectively. According to certain studies [27,28], all processes are affected by the contacts' characteristics. The solar cell's ability to produce its own internal electric field and the contact cathode/ETM and anode/HTM's ohmic or rectifying activity are both responsible for this result. In order to optimize the device performance the back contact domain is taken between 1 nm and 150,000 nm with a step of 50 nm. Fig. 7 presents the variation of *PCE* as a function of BMC thickness for three structures. From this figure, the optimum BMC thickness value is less than 50 nm.

Table 3 summarizes different layers and deposition Materials that appear frequently in top PCE cells by using ML techniques. From this table, we can notice that SnO_2 is frequently used in perovskite solar cells with a percentage of 33 % more than other materials this fact is due to its superior properties in terms of conductivity, transparency, and suitable band alignment. For the absorber layer, it is found that CsFAMAPbBrI outperforms other candidates like MAPbI and FAMAPbBrI. Because it has a high glass transition temperature (Tg), morphological stability, and is simple to produce while preserving strong electrical characteristics, Spiro-MeOTAD, which has a 20 % efficiency, surpasses materials like NiO_x and PTAA. Finally, Au as BMC shows 30 % and outperforms other metals like Ag. It is worth noticing that sometimes the sum of percentage in one layer is more than 100, because some materials appeared as the second layer, for example, PCBM-60 as ETL and C60 as the second layer. In other words, the number of material compositions (samples) is bigger than the number of materials. Therefore, the percentage only helps in ranking the best materials. Table 4 provides a comparison between our findings and the top experimental devices in our dataset.

The consensus of this ML model outcomes with a large amount of experimental data provides a good indication of the potential for advancement. Table 3 establishes favorable and clear guidance for experiments involving PCE improvement, reducing the large variety of different candidate materials.

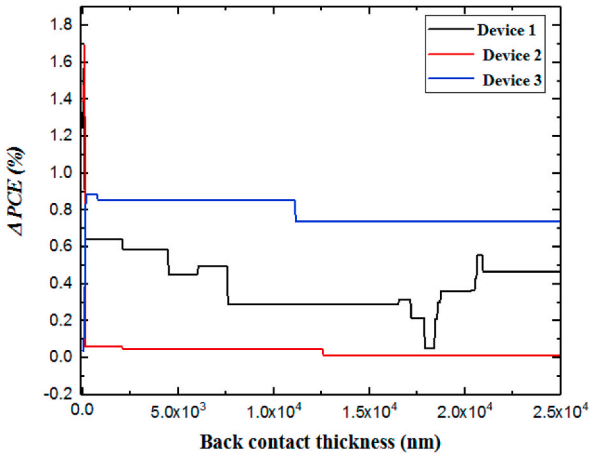

Fig. 7. Presents the variation of *PCE* as a function of BMC thickness.

Table 3
Different layer/deposition Materials that appear frequently in top PCE cells by using techniques.

Layers/deposition materials	Materials	Percentage	Total materials
ETL	SnO_2	33 %	262
	PCBM-60	27 %	
	BCP	25 %	
	C60	23 %	
	TiO_2	23 %	
Perovskite	CsFAMAPbBrI	22 %	120
	MAPbI	15 %	
	FAMAPbBrI	11 %	
HTL	Spiro-MeOTAD	20 %	385
	NiOx	10 %	
	PTAA	10 %	
Back Contact	Au	30 %	65
	Ag	26 %	
	Cu	26 %	
	MoO_3	21 %	
	Ti	17 %	
Deposition Materials	DMF + DMSO (+other)	60 %	67
	DMSO + GBL		
Deposition quenching media	Chlorobenzee	58 %	30
	Ether	30 %	
	Toluene	29 %	

Materials: the material component of this layer in high-efficiency PSCs.
Percentage: the number of current materials in top efficiency cells divided by the total materials in top cells.
Total materials: the number of different materials compositions predicted by machine learning.

Table 4
Comparison between our findings with previous experimental works in our dataset.

ETL	Perovskite	HTL	Back Contact	Deposition Materials	Deposition Solvent	PCE (%)	Ref.
SnO_2	CsFAMAPbBrI	Spiro-MeOTAD	Au	DMF + DMSO	Chlorobenzene	23	This
$SnO_{2+}In_2O_3$	FAMAPbIs	Spiro-MeOTAD	Au	DMF + DMSO + IPA	Unknown	23.07	[29]
TiO_2 + TiO_2-mp + PCBM-60+ PMMA + BAI	CsFAMAPbBrI	BAI + Spiro-MeOTAD	Au	DMF + DMSO	Chlorobenzene	22.77	[23]

4. Conclusion

In this work, an optimization strategy via Machine learning technique was adopted to boost the performance of perovskite solar cells. By using the Random Forest technique, 3000 samples of perovskite solar cells samples collected from previous experimental studies were examined and classified. The *PCE* of the solar cells was considered as the target (output). New perovskite solar cell

configurations were generated by the ML model. Fe_2O_3/CsPbBrI_2/NiO-mp/Carbon, CdS/FAMAPbI_3/NiO–C/Au and PCBM-60/Phen-NaDPO/MAPbI_3/asy-PBTBDT/Ag were the best new configurations with PCE exceeding 20 %. In addition, a thorough investigation of the impact of important parameters like perovskite bandgap, ETL thickness, thermal annealing temperature, and back contact thickness on device performance was performed. Our findings show that the optimized structure SnO_2/CsFAMAPbBrI/Spiro-OmeTAD/Au presents an efficiency of 23 %. Our primary emphasis in a subsequent study will be to decrease the time required and increase the capabilities of this approach while taking into account vast amounts of perovskite solar cell data that also contain extra environmental parameters.

Funding

Deanship of Scientific Research at King Khalid University, Saudi Arabia.

Data availability

Data will be made available on request.

CRediT authorship contribution statement

M. Mammeri: Writing – original draft, Data curation, Formal analysis, Software. **L. Dehimi:** Writing – review & editing, Formal analysis, Methodology, Validation. **H. Bencherif:** Conceptualization, Formal analysis, Software, Visualization, Writing – original draft, Writing – review & editing, Supervision. **Mongi Amami:** Resources, Validation, Visualization. **Safa Ezzine:** Funding acquisition, Validation, Visualization. **Rahul Pandey:** Formal analysis, Validation, Visualization. **M. Khalid Hossain:** Formal analysis, Funding acquisition, Project administration, Supervision, Validation, Visualization, Writing – review & editing.

Declaration of competing interest

The authors declare that they have no known competing financial interests or personal relationships that could have appeared to influence the work reported in this paper.

Acknowledgements

The authors have extended their appreciation to the Deanship of Scientific Research at King Khalid University, Saudi Arabia for funding this work through the Research Groups Program under grant number R.G.P.2: 233/44. The SCAPS-1D program was kindly provided by Dr. M. Burgelman of the University of Gent in Belgium. The authors would like to express their gratitude to him.

References

[1] J. Biamonte, P. Wittek, N. Pancotti, P. Rebentrost, N. Wiebe, S. Lloyd, Quantum machine learning, Nature 549 (7671) (2017) 195–202, https://doi.org/10.1038/nature23474.
[2] B. Mahesh, Machine learning algorithms-a review [Internet], Int. J. Sci. Res. 9 (1) (2020) 381–386.
[3] H. Bencherif, M.K. Hossain, Design and numerical investigation of efficient (FAPbI3) 1− x (CsSnI3) x perovskite solar cell with optimized performances, Sol. Energy 248 (2022) 137–148.
[4] M.K. Hossain, G.I. Toki, A. Kuddus, M.H.K. Rubel, M.M. Hossain, H. Bencherif, M. Mushtaq, An extensive study on multiple ETL and HTL layers to design and simulation of high-performance lead-free CsSnCl3-based perovskite solar cells, Sci. Rep. 13 (1) (2023) 2521.
[5] M.K. Hossain, G.I. Toki, J. Madan, R. Pandey, H. Bencherif, M.K. Mohammed, D.P. Samajdar, A comprehensive study of the optimization and comparison of cesium halide perovskite solar cells using ZnO and Cu 2 FeSnS 4 as charge transport layers, New J. Chem. 47 (18) (2023) 8602–8624.
[6] M. Khaouani, H. Bencherif, A. Meddour, Boosted perovskite photodetector performance using graphene as transparent electrode, Transactions on Electrical and Electronic Materials 23 (2) (2022) 113–121.
[7] M.K. Hossain, G.I. Toki, A. Kuddus, M.K. Mohammed, R. Pandey, J. Madan, D.P. Samajdar, Optimization of the architecture of lead-free CsSnCl3-perovskite solar cells for enhancement of efficiency: a combination of SCAPS-1D and wxAMPS study, Mater. Chem. Phys. (2023), 128281.
[8] M. Khaouani, H. Bencherif, Z. Kourdi, An improved perovskite solar cell employing InxGa1-xAs as an efficient hole transport layer, J. Comput. Electron. 22 (1) (2023) 394–400.
[9] NationalCenter for Photovoltaics at the National NREL, Research cell efficiency records, Available online: https://www.nrel.gov/pv/cell-efficiency.html.
[10] B. Yılmaz, R. Yıldırım, Critical review of machine learning applications in perovskite solar research, Nano Energy 80 (2021), 105546.
[11] Ç. Odabaşı, R. Yıldırım, Performance analysis of perovskite solar cells in 2013–2018 using machine-learning tools, Nano Energy 56 (2019) 770–791.
[12] C. Chen, A. Maqsood, T.J. Jacobsson, The role of machine learning in perovskite solar cell research, J. Alloys Compd. (2023), 170824.
[13] M. Mammeri, L. Dehimi, H. Bencherif, F. Pezzimenti, Paths towards high perovskite solar cells stability using machine learning techniques, Sol. Energy 249 (2023) 651–660.
[14] K. Kira, L.A. Rendell, The feature selection problem: traditional methods and a new algorithm, in: Proceedings of the Tenth National Conference on Artificial Intelligence, 1992, July, pp. 129–134.
[15] T.J. Jacobsson, A. Hultqvist, A. García-Fernández, A. Anand, A. Al-Ashouri, A. Hagfeldt, E. Unger, An open-access database and analysis tool for perovskite solar cells based on the FAIR data principles, Nat. Energy 7 (1) (2022) 107–115.
[16] A. Singh, N. Thakur, A. Sharma, A review of supervised machine learning algorithms, in: 2016 3rd International Conference on Computing for Sustainable Global Development, INDIACom, Ieee, 2016, March, pp. 1310–1315.
[17] V. Rodriguez-Galiano, M. Sanchez-Castillo, M. Chica-Olmo, M.J.O.G.R. Chica-Rivas, Machine learning predictive models for mineral prospectivity: an evaluation of neural networks, random forest, regression trees and support vector machines, Ore Geol. Rev. 71 (2015) 804–818.
[18] S. Nakagawa, H. Schielzeth, A general and simple method for obtaining R2 from generalized linear mixed-effects models, Methods Ecol. Evol. 4 (2) (2013) 133–142.

[19] G.S.K. Ranjan, A.K. Verma, S. Radhika, K-nearest neighbors and grid search cv based real time fault monitoring system for industries, in: 2019 IEEE 5th International Conference for Convergence in Technology (I2CT), IEEE, 2019, pp. 1–5.
[20] S.M. LaValle, J.J. Kuffner, B.R. Donald, Rapidly-exploring random trees: progress and prospects, Algorithmic and computational robotics: N. Dir. 5 (2001) 293–308.
[21] M.H. Kumar, N. Yantara, S. Dharani, M. Graetzel, S. Mhaisalkar, P.P. Boix, N. Mathews, Flexible, low-temperature, solution processed ZnO-based perovskite solid state solar cells, Chem. Commun. 49 (94) (2013) 11089–11091.
[22] L. Zuo, Z. Gu, T. Ye, W. Fu, G. Wu, H. Li, H. Chen, Enhanced photovoltaic performance of CH3NH3PbI3 perovskite solar cells through interfacial engineering using self-assembling monolayer, J. Am. Chem. Soc. 137 (7) (2015) 2674–2679.
[23] M.A. Mahmud, et al., Origin of efficiency and stability enhancement in high performing mixed dimensional 2D-3D perovskite solar cells: a Review, Adv. Funct. Mater. 32 (3) (2021), 2009164, https://doi.org/10.1002/adfm.202009164.
[24] J.J. Yoo, et al., An interface stabilized perovskite solar cell with high stabilized efficiency and low voltage loss, Energy & Environmental Science 12 (7) (2019) 2192–2199, https://doi.org/10.1039/c9ee00751b.
[25] D. Liu, T.L. Kelly, Perovskite solar cells with a planar heterojunction structure prepared using room-temperature solution processing techniques, Nat. Photonics 8 (2) (2014) 133–138.
[26] J. Zhou, X. Meng, X. Zhang, X. Tao, Z. Zhang, J. Hu, S. Yang, Low-temperature aqueous solution processed ZnO as an electron transporting layer for efficient perovskite solar cells, Mater. Chem. Front. 1 (5) (2017) 802–806.
[27] H. Bencherif, L. Dehimi, N. Mahsar, E. Kouriche, F. Pezzimenti, Modeling and optimization of CZTS kesterite solar cells using TiO2 as efficient electron transport layer, Mater. Sci. Eng., B 276 (2022), 115574.
[28] H. Bencherif, F. Meddour, M.H. Elshorbagy, M.K. Hossain, A. Cuadrado, M.A. Abdi, J. Alda, Performance enhancement of (FAPbI3) 1-x (MAPbBr3) x perovskite solar cell with an optimized design, Micro and Nanostructures 171 (2022), 207403.
[29] P. Wang, et al., Gradient energy alignment engineering for planar perovskite solar cells with efficiency over 23%, Adv. Mater. 32 (6) (2020) https://doi.org/10.1002/adma.201905766.